Differential electrophysiological response during rest, self-referential, and non–self-referential tasks in human posteromedial cortex

Mohammad Dastjerdi[a,b], Brett L. Foster[a,b], Sharmin Nasrullah[a,b], Andreas M. Rauschecker[a,c,d], Robert F. Dougherty[d], Jennifer D. Townsend[a,b], Catie Chang[e], Michael D. Greicius[b,f], Vinod Menon[b,f], Daniel P. Kennedy[g], and Josef Parvizi[a,b,1]

[a]Laboratory of Behavioral and Cognitive Neurology, Departments of [b]Neurology and Neurological Sciences, [d]Psychology, [e]Electrical Engineering, and [f]Psychiatry and Behavioral Sciences, and [c]Neurosciences Graduate Program and Medical Scientist Training Program, Stanford University, Stanford, CA 94305; and [g]Division of Humanities and Social Sciences, California Institute of Technology, Pasadena, CA 91125

Edited* by Marcus E. Raichle, Washington University of St. Louis, St. Louis, MO, and approved December 29, 2010 (received for review November 13, 2010)

The electrophysiological basis for higher brain activity during rest and internally directed cognition within the human default mode network (DMN) remains largely unknown. Here we use intracranial recordings in the human posteromedial cortex (PMC), a core node within the DMN, during conditions of cued rest, autobiographical judgments, and arithmetic processing. We found a heterogeneous profile of PMC responses in functional, spatial, and temporal domains. Although the majority of PMC sites showed increased broad gamma band activity (30–180 Hz) during rest, some PMC sites, proximal to the retrosplenial cortex, responded selectively to autobiographical stimuli. However, no site responded to both conditions, even though they were located within the boundaries of the DMN identified with resting-state functional imaging and similarly deactivated during arithmetic processing. These findings, which provide electrophysiological evidence for heterogeneity within the core of the DMN, will have important implications for neuroimaging studies of the DMN.

electrocorticography | oscillations | posterior cingulate | precuneus

Functional neuroimaging studies have consistently shown that a specific network of brain regions, known as the default mode network (DMN), has reduced hemodynamic activity during the performance of externally directed attention tasks (1–5), while having higher activity during resting states and internally focused self-referential tasks (4, 6–8). Thus, an intriguing idea has emerged that increased activity in the DMN during rest may reflect internally focused self-referential cognition (9–13). However, it is still unclear whether the overlapping imaging activity of resting and self-referential processing reflects shared or distinct neurophysiological activity. Are the same regions within the DMN active during rest *and* self-referential processing?

To date, our understanding of the functional operation of the DMN is predominantly derived from studies using neuroimaging methods, which have limited temporal resolution. In addition, the spatial resolution of imaging methods are often reduced by spatial smoothing, intersubject spatial normalization, and reliance on group analysis—all of which may obscure the anatomical localization of functional responses (14). Because electrophysiological activity associated with the DMN is mostly hidden within the medial cortical surface, it is typically not detected at the scalp with standard electroencephalography. Moreover, intracranial electrophysiological recordings in the interhemispheric space of the brain in clinical subjects are also rare. Thus, the neurophysiological correlates and temporal dynamics of DMN activity during rest or cognitive tasks remain to be explored using methods that have higher temporal resolution and individualized anatomical precision (15).

In the present study, we performed multielectrode intracranial recordings from the human posteromedial cortex (PMC), the central hub of the DMN (refs. 16–18; Fig. 1), in four epilepsy patients. It should be noted that the ability to obtain intracranial recordings from the human PMC using multielectrode coverage is quite exceptional because this region of the brain is rarely targeted for epilepsy surgery. In all four subjects, the implantation of electrodes was solely for the purpose of presurgical evaluation to help localize the seizure onset zone. Details about the location of seizure-onset zone in each subject are described in Fig. 1.

All subjects also underwent resting-state functional MRI (rsfMRI) before their implantation with intracranial electrodes (Fig. 1) to localize the DMN. After implantation, subjects were monitored over several days while awake and comfortable in their hospital rooms. During this time, we administered a cognitive task that was repeated twice in each subject.

The experiment was designed to compare the activity of PMC and non-PMC regions during rest, self-referential processing, and mathematical processing. We addressed the following two aims: (*i*) to test whether there is a significant change of electrophysiological activity within all or only specific subregions of the human PMC during resting compared with self-related and non-self-related task conditions and to compare the temporal profile of changes in activity under these conditions; and (*ii*) to determine whether the sites within the PMC that are active during rest also show similar changes in electrophysiological activity during self-referential processing.

Electrophysiological data were recorded while subjects participated in an experimental task that involved three main conditions (19). For two conditions, participants had to respond "true" or "false" to either simple arithmetic equations (*math condition*, e.g., "59 + 7 = 66") or self-referential autobiographical statements (*autobiographical condition*, e.g., "I used a computer today"). (Subject 3 was non-English-speaking and did not perform autobiographical judgments). The third condition involved randomly occurring 5-s resting events during which subjects were instructed to rest when a visual cue appeared (*rest condition*; Fig. S1). In subjects 1 and 2, we also presented statements about their own personal attributes and asked the subjects to respond "true" or "false." These self-referential stimuli were either about personal internal attributes (*self-internal condition*, e.g., "I am honest") or about external attributes (*self-external condition*, e.g., "I usually wear white socks"). Finally, we recorded data during 3-min resting blocks in which subjects were asked to lie still in their bed and rest with eyes open and closed.

Author contributions: J.P. designed research; M.D., B.L.F, S.N., A.M.R., C.C., and J.P. performed research; R.F.D., M.D.G., V.M., D.P.K., and J.P. contributed new reagents/analytic tools; M.D., B.L.F., S.N., A.M.R., J.D.T., and J.P. analyzed data; and M.D., B.L.F., and J.P. wrote the paper.

The authors declare no conflict of interest.

This article is a PNAS direct submission.

*This Direct Submission article had a prearranged editor.

[1]To whom correspondence should be addressed. E-mail: jparvizi@stanford.edu.

This article contains supporting information online at www.pnas.org/lookup/suppl/doi:10.1073/pnas.1017098108/-/DCSupplemental.

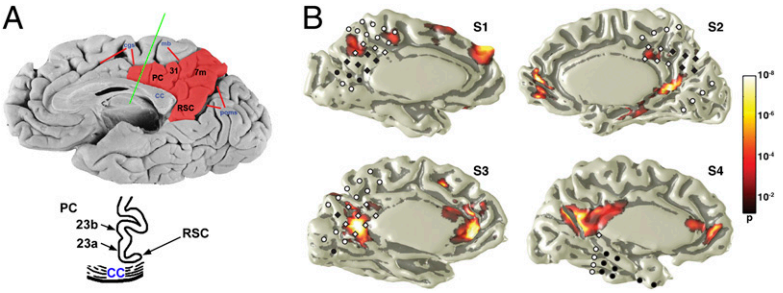

Fig. 1. The PMC boundaries and fMRI/electrode location. (*A*) The PMC includes posterior cingulate [PC; i.e., Brodmann areas (BA) 23a and 23b], and retrosplenial cortex (RSC; BA29/30), along with medial parietal BA 31 and 7 m. The RSC extends anteriorly in the depth of the callosal sulcus adjacent and lateral to the PC area BA23a up to the midcingulate level, as shown in the sketch of the coronal section of the brain from the level of the midcingulate gyrus (green line). The boundaries of the PMC are easily defined by the corpus callosum (cc), the marginal branch (mb) of the cingulate sulcus (cgs), and the parieto-occipital medial sulcus (poms). These anatomical boundaries were used for classifying electrodes as PMC or non-PMC. (*B*) Medial view of the DMN derived from independent component analysis (color bar reflects significance of voxel correlation with selected component) of rsfMRI data and location of intracranial electrodes in each of the four subjects (s1–s4). PMC electrodes are shown as diamonds (non-PMC as circle); all excluded electrodes are indicated with black fill. The seizure onset zone was found to be located in the depth of parieto-occipital sulcus (subject 1), cuneus (subject 2), LPC (subject 3), and posterior temporal region (subject 4).

The same experimental task was recently used in an fMRI study of the DMN in normal controls and patients with autism, and the authors reported higher blood oxygen level dependent (BOLD) response within the PMC during rest and self-referential tasks compared with the math condition and found that an overlap of activity during self-referential and rest conditions was seen in the ventral PMC region (19).

Results

We classified electrodes as PMC sites if they were located within the anatomical boundaries of the PMC as defined in Fig. 1*A*, with all other sites classified as non-PMC. Of those sites classified as PMC, a subset were observed to overlap with the DMN identified with rsfMRI (Fig. 1*B*). In order to visualize electrophysiological response, we created event-related spectral perturbation (ERSP) maps based on the normalized power of electrophysiological activity during each condition. We subsequently focused our analysis on the changes in broad (low and high) gamma power (GP)—i.e., within 30–180 Hz (see *SI Methods* for details). To quantify the change in GP for each electrode, we used estimates of relative GP, which reflects the magnitude of GP change relative to the overall mean GP during the entire experiment.

Increased PMC Activity in the Broad Gamma Band Range During Cued Rest. We found higher GP in the 30- to 180-Hz range in the PMC during cued rest. This higher activity peaked shortly after the onset of the cue and persisted throughout the entire 5 s of cued rest for most PMC sites; by comparison, a significantly different pattern of activity was seen in some of the non-PMC electrodes, such as the lateral parietal cortex (LPC), where only a short and transient increase of GP was seen after the resting cue (Fig. 2 and Fig. S2).

The general trend of increased relative GP in PMC during rest did not change statistically as a function of whether the resting event was brief (5 s) or continuous over an extended 3-min block including both eyes open and closed [$F(2, 651) = 1.2$, $P = 0.3$; two-way ANOVA; Fig. S3]. The relative GP during all three conditions was significantly higher in PMC than in non-PMC [$F(1, 651) = 24.2$, $P < 0.001$; two-way ANOVA].

Temporal Profile of Response During Cued Rest. To study the temporal evolution of gamma activity during cued rest, we compared the change of relative GP during transitions between nonrest and rest conditions in PMC electrodes. As seen in Fig. 3*A*, the relative GP sharply increased as the condition changed from nonrest to rest and remained above the overall mean GP throughout the entire resting event and during the initial transition from rest to nonrest before returning below the overall mean GP (Fig. 3 *A* and *B*). The same result was not seen in subject 4's PMC electrode (Fig. 3*A*, gray trace), which showed minor fluctuations of relative GP around the overall mean GP during rest, but a significantly increased relative GP during the autobiographical condition (see below).

We calculated the response onset latency of relative GP after the onset of the rest cue and found that the rise of gamma activity

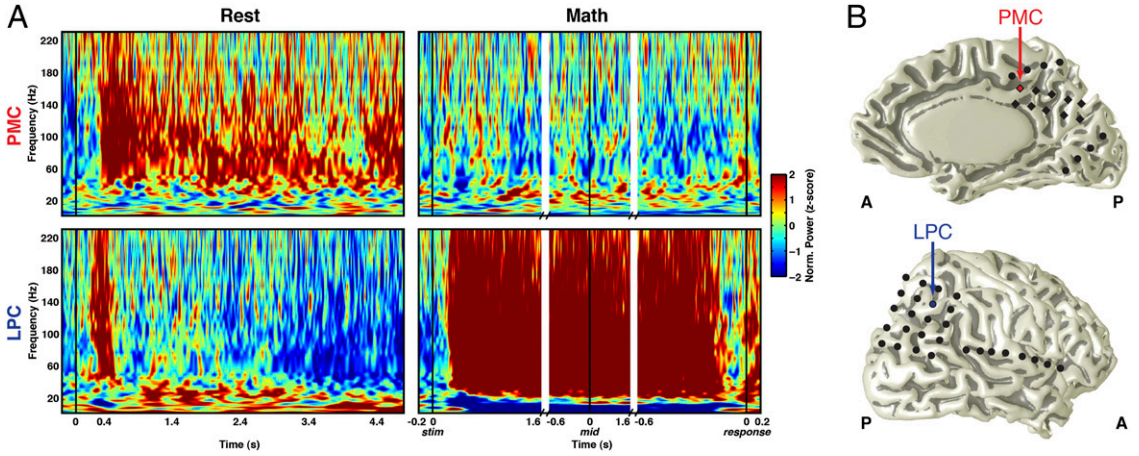

Fig. 2. Differential electrophysiological response in the PMC and non-PMC during rest and math conditions. (*A*) ERSP maps during rest and math conditions for electrodes located within the right PMC and LPC in subject 2. (*B*) Across trials, GP increased in the PMC 384 ± 138 ms (median ± SE) after the onset of rest cue and persisted throughout the trial (5 s), whereas the LPC showed only a transient increase in GP of 318 ± 217 ms after the onset of rest cue. During the math condition, the PMC showed decreased GP, whereas the LPC displayed an increase in GP 257 ± 40 ms after the onset of math stimuli until it ended shortly before the subject responded. ERSPs during the math task are aligned to the time of stimulus onset (stim), the midpoint of onset-to-response-time (mid), and the time of response (response).

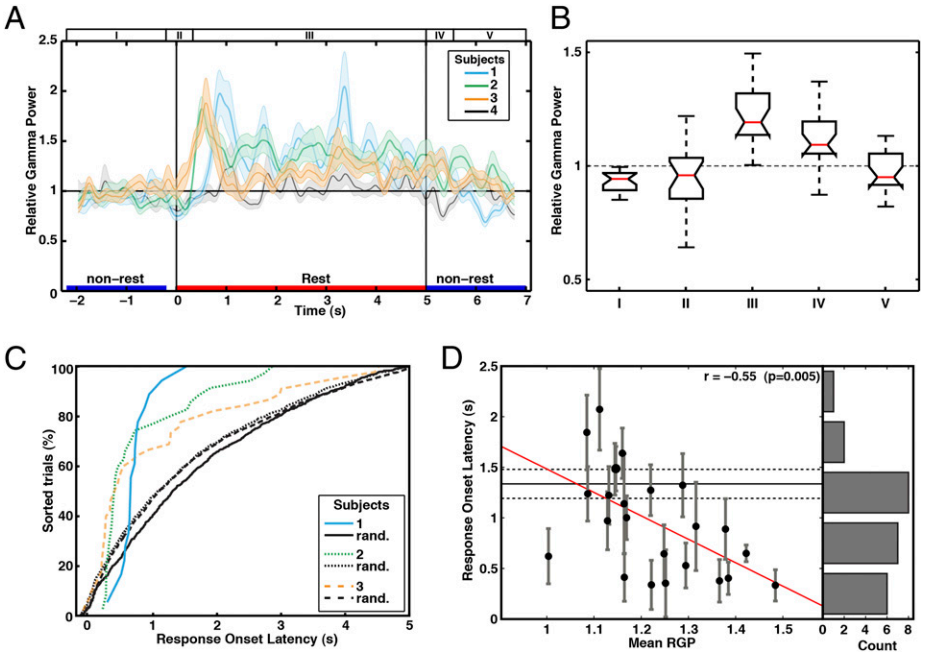

Fig. 3. Temporal profile of broad gamma activity during transitions between nonrest and rest. (*A*) The temporal profile of relative GP (RGP) change in a representative PMC electrode for all subjects and averaged across two experiments. On the *y* axis the overall mean GP has a value of 1. The shading around each trace is the SE of RGP. The green trace belongs to the electrode shown in Fig. 2*A*, and the gray trace belongs to the only PMC electrode in subject 4. (*B*) Boxplot values for the RGP in five different epochs of transition between nonrest and rest for the 12 of 17 PMC electrodes with major increase of GP (see below). Each boxplot reflects the median (central notch mark), 25th, and 75th percentiles (upper and lower box edges), with whiskers extending to minimum and maximum values (medians are significantly different at $P = 0.05$ if notch widths do not overlap). These epochs, which are marked I–V in *A*, were as follows: (I) last 2 s of nonrest; (II) transition from nonrest to rest (200-ms black screen and 300-ms rest cue); (III) remaining rest period (4.7 s); (IV) 500 ms of transition from rest to nonrest (without ISI; Fig. S1); and (V) 1.5 s of nonrest. (*C*) The response onset latency values for the traces in subjects 1–3. Trials are sorted according to their response onset latency values in cumulative distribution. Each point on the curve represents the time of GP rise for one trial. The latency values for each of the three traces is significantly shorter than the corresponding random latency (black curves; $P < 0.001$; Wilcoxon rank test). (*D*) Distribution of latency values vs. mean RGP (in two experiments) for all PMC electrodes with increased gamma activity during rest. The counts of response onset latency values (*Right*) suggest that the majority of electrodes had shorter latency than the mean random latency (horizontal solid black line) ± SD (dashed lines).

in the PMC was locked to the appearance of the rest cue for the majority of trials (Fig. 3*C*). In PMC electrodes with increased GP during rest, the relative GP was locked to the resting cue onset, with different median values of response onset latency across subjects (Fig. 3*C*). Interestingly, a significant negative correlation was found between mean relative GP and latency during rest, suggesting that, in general, electrodes that showed higher gamma activity during rest responded faster during the transition from nonrest to rest ($r = -0.55$, $P < 0.01$; Fig. 3*D*).

Spatial Heterogeneity of Electrophysiological Response Within the PMC. To measure the change of activity on the same scale across all electrodes and subjects, we defined a differential activity index (DAI) as the normalized difference between the mean GP of an electrode during a condition and its overall mean GP during all conditions. Thus, a positive DAI in an electrode during a given condition would signify higher gamma-band activity during that particular condition compared with its overall mean GP. The distribution of DAI values for PMC electrodes was shifted positive during rest and negative during math, but was around zero for the autobiographical condition in comparison with non-PMC (Fig. 4 *A*–*C*, red curve). Interestingly, the DAI values even among adjacent PMC electrodes differed in magnitude, suggesting a possible nonuniform spread of rest responses over the PMC (Fig. 4*E*). The small number of PMC electrode locations across subjects make it difficult to conclude much about the anatomical specificity of the response.

As can be noted in Fig. 1*B*, the delineation of the fMRI-defined PMC hub of the DMN appeared to vary between subjects. This variability may be explained in part by normal individual variability, or it may be related to the proximity of the pathological epileptic zone to the PMC in our clinical cohort, especially in subject 1 (Fig. 1). Despite the individual rsfMRI differences, what is striking in our findings is the spatial overlap between the hubs of resting electrophysiological and fMRI activities in each subject. As shown in Fig. 4*E*, the strongest electrocorticography (ECoG) responses during rest overlapped with the rsfMRI components of the DMN within the PMC in each subject. Therefore, although rsfMRI anatomy differed between subjects, so did the location of peak electrophysiology response; however, importantly, both overlapped within each subject.

Functional Heterogeneity of Electrophysiological Response Within the PMC. We compared the functional properties of PMC and non-PMC regions across different task conditions and found a significant interaction between task condition (rest, math, autobiographical) and electrode location (PMC/non-PMC) [$F(2, 615) = 34.75$, $P < 0.001$]. The mean DAI for PMC electrodes differed significantly from non-PMC electrodes during rest and math but not the autobiographical condition (Fig. 5*A*). However, two PMC electrodes (one each from subjects 2 and 4, close to or within the retrosplenial cortex) had significantly higher gamma activity during the autobiographical condition (Figs. 5*B* and 6 and Fig. S4). These sites did not show a significant change of gamma activity during rest, but had significantly decreased activity during the math condition (Figs. 5*B* and 6). In 12 of 17 PMC electrodes (compared with 7 of 98 non-PMC electrodes), the positive resting DAI values were in excess of at least 1 SD (Fig. 5*C*). As a confirmation, we used this criterion to blindly select electrodes responsive to the rest condition (all subjects) and found the stereotaxic Talairach location of these selected sites to cluster within the PMC region (red electrodes in Fig. 5*D*). Conversely, the electrodes with negative resting DAI values in excess of at least 1 SD (blue electrodes in Fig. 5*D*) were located mostly on the lateral surface of the brain.

To explore relationship between response magnitudes across conditions, we plotted the relative GP values for each electrode during two different conditions. We found a significant negative correlation between the responses during math and rest condition (Fig. 5*E*), meaning that the electrodes with higher activity during rest showed greater deactivation during math. However, no significant correlation was found between the relative GP during autobiographical and rest conditions (Fig. 5*F*). As noted above, two electrodes in two subjects had significantly high relative GP during autobiographical processing (marked by gray circles in Fig. 5*F*). These electrodes were within or proximal to the retrosplenial cortex. Temporally, the profile of responses for these two electrodes was comparatively late compared with other PMC elec-

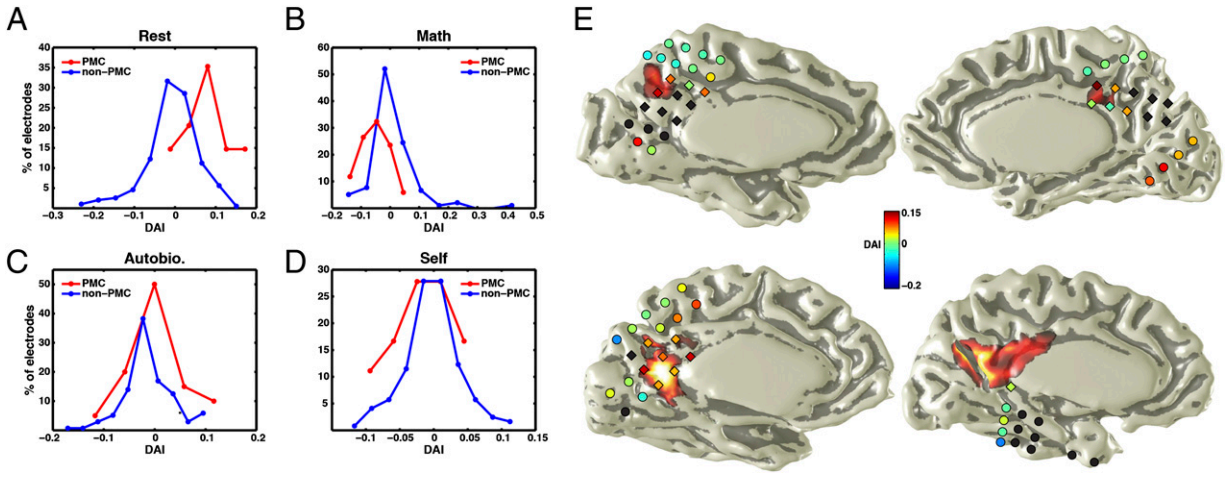

Fig. 4. The DAI distribution. (*A–D*) The distribution of DAI values for PMC and non-PMC electrodes during rest (*A*), math (*B*), autobiographical (*C*), and self (internal and external) (*D*) conditions for all experiments. The DAI of most PMC electrodes is positive during rest (*A*) and negative during math condition (*B*). The DAI values in PMC and non-PMC electrodes are not different during autobiographical or self-internal/external conditions and are distributed around zero. (*E*) The color of each electrode denotes DAI during rest in each of the four subjects. PMC electrodes are shown as diamonds (non-PMC as circle); all excluded electrodes are indicated with black fill.

trodes with similar response magnitude (DAI) to only the rest condition (Fig. 6 and Fig. S4).

It should be noted that the sites responsive to the autobiographical condition were strongly inactive during the math condition (Fig.6*C* and Fig. S4*C*), which also involved button responses. Moreover, sites responsive to the autobiographical condition were distal from any primary or supplementary motor areas. These results suggest that the differential response during autobiographical condition cannot be due to motor (i.e., key press) factors. On a side note, in subjects with electrodes on motor or somatosensory cortex, the activity at these sites did not show any preparatory gamma response during the autobiographical condition; rather, they only showed increased gamma just before response.

In two subjects, we were able to further examine the response of all electrodes during self-internal or self-external conditions. In these subjects, no PMC electrodes active during rest were

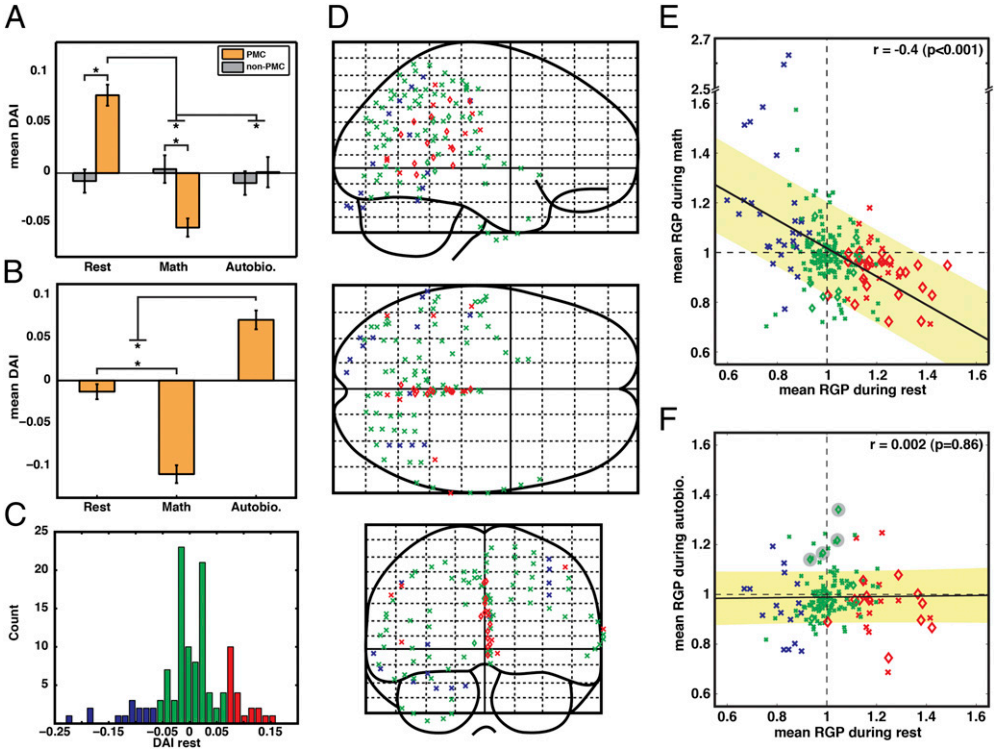

Fig. 5. Regional and functional specificity of gamma activity. (*A*) There was a significant interaction between task condition and electrode location. Mean DAI of PMC compared with non-PMC electrodes is significantly higher during rest, significantly lower during math, and not significantly different during the autobiographical condition (*$P < 0.003$, Bonferroni corrected). Although *A* shows the results of group analysis, the same profile holds for the PMC in each subject. (*B*) Two PMC electrodes (one each from subjects 2 and 4) had significantly higher activity during the autobiographical condition compared with rest and math (*$P < 0.02$, Bonferroni corrected). Both electrodes were located in the ventral posterior cingulate gyrus in ventral BA23a (subject 2; Fig. S4) and BA29/30 (subject 4; Fig. 6). (*C*) The histogram of DAI values is shown for all electrodes during the rest condition (two experiments). We assigned red or blue colors to the DAI values 1 SD greater or less than the mean, respectively, with the remainder set to green. (*D*) Location of all electrodes in all subjects on a spatially normalized glass brain in Talairach space colored with respect to the rest DAI values as defined in *C* (PMC, diamonds; non-PMC, x). (*E* and *F*) For all electrodes and in all experiments, the RGP was plotted during rest vs. math (*E*) or rest vs. autobiographical condition (*F*). Color convention in *E* and *F* is the same as in *C* and *D*. The value of 1 on horizontal and vertical axes in *E* and *F* denotes the overall mean GP during that condition. Note that in *E*, PMC electrodes (diamonds) fall in the right lower quadrant; i.e., they are active during rest (right of vertical axis of 1) and deactivated during math (below the horizontal axis of 1). The solid black line with the yellow band shows the regression line with its SE. Four gray markers in *F* denote electrodes in *B* (two sites and two experiments).

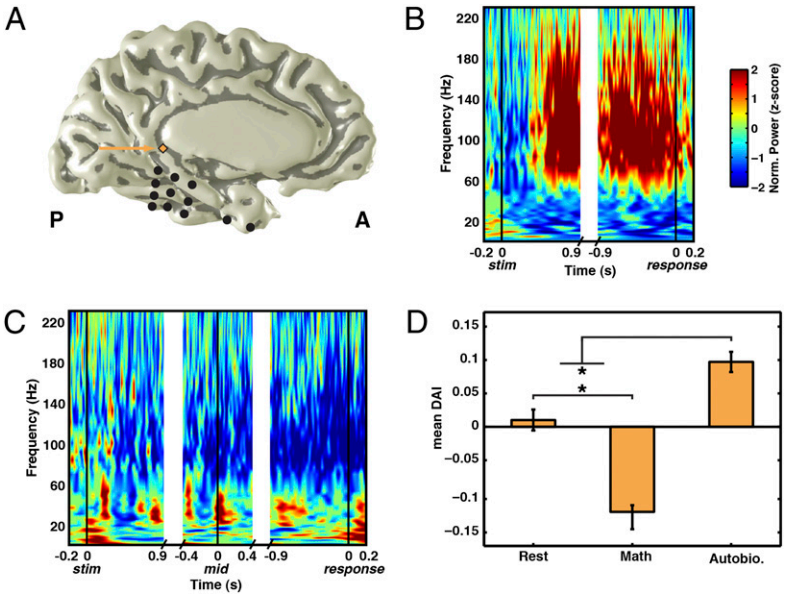

Fig. 6. Broad gamma activity in the PMC during autobiographical condition. (*A–C*) ERSP plots for a PMC electrode (*A*) during autobiographical (*B*) and math (*C*) conditions (subject 4). The location of the PMC electrode (diamond) is proximal to the retrosplenial cortex as outlined in Fig 1. ERSPs are aligned as per Fig. 1. (*D*) Mean DAI for this electrode across all presented conditions. The mean DAI was significantly different across conditions [$F(2,237) = 51.97$ $P < 0.001$] with the autobiographical condition being significantly higher than rest and math conditions, which were also significantly different (*$P <$ 0.02, Bonferroni corrected).

active during either self-internal or self-external conditions (Fig. S2). In addition, the distribution of DAI for both PMC and non-PMC electrodes centered around zero (Fig. 4*D*). Furthermore, in a comparison of rest condition to either of the two conditions for all electrodes, we found no correlation between relative GP during rest and self-internal ($r = -0.004$, $P = 0.96$) or self-external ($r = -0.12$, $P = 0.17$) conditions; conversely, there was a significant correlation between the relative GP during autobiographical and self-internal ($r = 0.62$, $P < 0.001$) as well as self-external ($r = 0.7$, $P < 0.001$) conditions (Fig. S5).

Discussion

Based on a large body of evidence (20–25), task-induced broad gamma band activity in a cortical region is an indication of higher local neural activity, which may include both synaptic and spiking events. Thus, our findings provide clear electrophysiological evidence that the human PMC has significantly higher neural activity during rest, whereas it is deactivated by attentionally demanding tasks such as arithmetic processing—a finding that is consistent with neuroimaging work.

Furthermore, our findings also extend recent evidence from functional imaging studies of the DMN and the recent electrophysiological findings in nonhuman primate (26) and human (15, 27) PMC. We found a remarkably heterogeneous profile of response within the PMC. Although some PMC sites showed a strong response to the rest cue, others responded selectively to autobiographical self-referential stimuli—yet none responded to both conditions, even though they were similarly deactivated during the attentionally demanding math condition. In the spatial domain, the electrodes responsive to the autobiographical stimuli were in the most ventral portion of the PMC, close to the retrosplenial cortex, which also extends anteriorly in the depth of the callosal sulcus and lateral to the posterior cingulate area 23a (Fig. 1*A*). In the temporal domain, functionally different electrodes showed differing profiles of response. For instance, whereas the response to the rest cue was early and peaked at its onset, the response to autobiographical stimuli was comparatively late.

Together, these findings are in line with the anatomical heterogeneity described in the nonhuman (28) and human (29) PMC, and they support the idea that the DMN might be functionally heterogeneous (13, 29, 30). On the basis of these findings, we hypothesize that the PMC sites responsive to autobiographical self-referential stimuli might be engaged in memory network activity during spontaneous cognition or introspection (31), whereas the sites responsive to the rest cue may have different functional significance.

Although we cannot be fully certain that patients did not engage in various kinds of cognitive processing during cued rest, there are several reasons to believe that the resting-evoked activity is unlikely to be due to the processing of a specific cognitive content per se. If patients were engaging in either autobiographical or mathematical cognition during cued rest, there should not be a divergence of response across conditions as seen in Fig. 4 *A* and *B*. Moreover, as shown in Fig. 4 *E* and *F*, relative GP was negatively correlated between the rest and math conditions and not correlated between rest and autobiographical conditions. Similarly, there was no correlation between relative GP during rest and self-referential conditions (Fig. S5). More importantly, the peak of gamma activity during rest occurs with short latency and is time-locked to the rest cue, with the same pattern of resting evoked activity seen across experiments conducted on different days. This stereotypy of response suggests that the resting evoked activity is less likely to be triggered by a specific cognitive content. The fact that the resting gamma activity is time-locked to the onset of the rest cue, rapid, and consistent across trials and experiments suggests that it may signal attentional disengagement rather than any specific conscious thinking.

The fMRI literature suggests that the DMN exists in a dynamic equilibrium with one or more additional networks linked to functions such as salience detection and executive control (3, 18, 32, 33). The temporal and spatial details of this interplay between the rest active PMC sites and nodes in these other networks require future exploration.

Methods

Subjects. The study was carried out entirely at the Laboratory of Behavioral and Cognitive Neurology at Stanford University Medical Center and involved four patients (three female and one male; mean age 33.5 y) with refractory epilepsy who were implanted with grid and/or strip electrodes on the medial and lateral surface of the brain (three with left hemisphere and one with right hemisphere coverage). Patient involvement in the study was based on informed voluntary consent and was part of an existing research protocol approved by the Stanford University Institutional Review Board office. Patients were not implanted for the purpose of our study, but only as part of a presurgical evaluation to help localize the seizure onset zone.

Of the 226 recorded electrodes, 124 were dual-sided and located on the medial surface of the brain (i.e., 62 facing the cortical surface and the other 62 making contact with the meninges of the contralateral hemisphere). Our prior experience with the dual-sided electrodes is that the contralateral-facing electrodes are significantly affected by the activity in the ipsilateral

hemisphere. Therefore, we elected to exclude 62 contralateral-facing electrodes from our quantitative analysis. We further excluded 49 electrodes because of epileptic activity or excessive artifacts.

Of the remaining 115 electrodes, which were entirely void of epileptic activity or artifacts, 17 electrodes were located in the anatomical region of the PMC and 98 in the non-PMC regions (Figs. 1*A* and 3*D*). The number of electrodes in each subject was 4, 5, 7, and 1 for PMC and 26, 35, 30, and 7 for non-PMC electrodes in subjects 1–4, respectively. Because our analysis focuses on differences between locations (PMC or non-PMC) and conditions (rest, math, autobiographical), each electrode contributes equally and individually to any analysis. Therefore, the inclusion of subject 4's single electrode to the PMC group should contribute no differently from any other electrode included in the analysis. In our analysis, electrodes are in no way weighted as a function of the total number of electrodes for any given location (PMC/non-PMC) or any given patient.

Task Conditions. ***Math condition.*** Subjects were shown math equations (addition only, e.g., "59 + 7 = 68") and were instructed to respond with a keypad button press as to whether the equation was true or false. Trial length was determined by the subject's reaction time. The mean reaction time was 4.3 ± 2.45 s (n = 8; four subjects with two experiments each).

Rest condition. Subjects passively viewed a plus sign that appeared on the center of black screen for 5 s and were told to rest and provide no response ("do nothing and let your mind wander").

Autobiographical condition. Subjects reviewed autobiographical statements and responded with keypad button presses as to whether the sentence was true or false (19). As in the math condition, trial length varied according to the subject's reaction time. The mean reaction time was 2.3 ± 0.98 s (n = 6; three subjects with two experiments each). As noted above, the experiment in subject 3 did not include the autobiographical condition because of lack of sufficient English knowledge.

In two subjects, we also presented other self-referential statements and asked the subjects to respond true or false with the keypad buttons. These self-referential stimuli were either about personal internal attributes (*self-internal condition*) or about external attributes (*self-external condition*). The mean reaction times for self-internal and self-external conditions were 2.4 ± 0.63 and 2.7 ± 0.77 s, respectively (n = 4; two subjects with two experiments each).

A list of all stimuli and details describing data analysis, electrophysiological data acquisition and preprocessing, ERSP, DAI and relative GP, and response onset latency time can be found in *SI Methods*.

ACKNOWLEDGMENTS. We thank the patients for participating in this study; Robert Knight and his laboratory members at the University of California, Berkeley, for their assistance with data analysis and useful comments on the manuscript; and Anthony Wagner, Brian Wandell, Bill Newsome, and their laboratory members at Stanford University for their insightful comments throughout the study. This work was supported by a grant from the Milken Family Foundation (to J.P) and by the Stanford University BioX program.

1. Shulman GL, et al. (1997) Common blood flow changes across visual tasks: II. Decreases in cerebral cortex. *J Cogn Neurosci* 9:648–663.
2. Raichle ME, et al. (2001) A default mode of brain function. *Proc Natl Acad Sci USA* 98: 676–682.
3. Fox MD, et al. (2005) The human brain is intrinsically organized into dynamic, anticorrelated functional networks. *Proc Natl Acad Sci USA* 102:9673–9678.
4. Buckner RL, Andrews-Hanna JR, Schacter DL (2008) The brain's default network: Anatomy, function, and relevance to disease. *Ann N Y Acad Sci* 1124:1–38.
5. Greicius MD, Srivastava G, Reiss AL, Menon V (2004) Default-mode network activity distinguishes Alzheimer's disease from healthy aging: evidence from functional MRI. *Proc Natl Acad Sci USA* 101:4637–4642.
6. Svoboda E, McKinnon MC, Levine B (2006) The functional neuroanatomy of autobiographical memory: a meta-analysis. *Neuropsychologia* 44:2189–2208.
7. Schacter DL, Addis DR, Buckner RL (2007) Remembering the past to imagine the future: The prospective brain. *Nat Rev Neurosci* 8:657–661.
8. Spreng RN, Mar RA, Kim AS (2009) The common neural basis of autobiographical memory, prospection, navigation, theory of mind, and the default mode: A quantitative meta-analysis. *J Cogn Neurosci* 21:489–510.
9. Summerfield JJ, Hassabis D, Maguire EA (2009) Cortical midline involvement in autobiographical memory. *Neuroimage* 44:1188–1200.
10. Northoff G, Bermpohl F (2004) Cortical midline structures and the self. *Trends Cogn Sci* 8:102–107.
11. Johnson SC, et al. (2002) Neural correlates of self-reflection. *Brain* 125:1808–1814.
12. Andreasen NC, et al. (1995) Remembering the past: Two facets of episodic memory explored with positron emission tomography. *Am J Psychiatry* 152:1576–1585.
13. Andrews-Hanna JR, Reidler JS, Sepulcre J, Poulin R, Buckner RL (2010) Functional-anatomic fractionation of the brain's default network. *Neuron* 65:550–562.
14. Van Essen DC, Dierker DL (2007) Surface-based and probabilistic atlases of primate cerebral cortex. *Neuron* 56:209–225.
15. Jerbi K, et al. (2010) Exploring the electrophysiological correlates of the default-mode network with intracerebral EEG. *Front Syst Neurosci* 4:27.
16. Hagmann P, et al. (2008) Mapping the structural core of human cerebral cortex. *PLoS Biol* 6:e159.
17. Gusnard DA, Raichle ME, Raichle ME (2001) Searching for a baseline: functional imaging and the resting human brain. *Nat Rev Neurosci* 2:685–694.
18. Fransson P, Marrelec G (2008) The precuneus/posterior cingulate cortex plays a pivotal role in the default mode network: Evidence from a partial correlation network analysis. *Neuroimage* 42:1178–1184.
19. Kennedy DP, Courchesne E (2008) Functional abnormalities of the default network during self- and other-reflection in autism. *Soc Cogn Affect Neurosci* 3:177–190.
20. Buzsaki G (2006) *Rhythms of the Brain* (Oxford University Press, London).
21. Jensen O, Kaiser J, Lachaux JP (2007) Human gamma-frequency oscillations associated with attention and memory. *Trends Neurosci* 30:317–324.
22. Lachaux JP, et al. (2005) The many faces of the gamma band response to complex visual stimuli. *Neuroimage* 25:491–501.
23. Crone NE, Miglioretti DL, Gordon B, Lesser RP (1998) Functional mapping of human sensorimotor cortex with electrocorticographic spectral analysis. II. Event-related synchronization in the gamma band. *Brain* 121:2301–2315.
24. Ray S, Crone NE, Niebur E, Franaszczuk PJ, Hsiao SS (2008) Neural correlates of high-gamma oscillations (60-200 Hz) in macaque local field potentials and their potential implications in electrocorticography. *J Neurosci* 28:11526–11536.
25. Manning JR, Jacobs J, Fried I, Kahana MJ (2009) Broadband shifts in local field potential power spectra are correlated with single-neuron spiking in humans. *J Neurosci* 29: 13613–13620.
26. Hayden BY, Smith DV, Platt ML (2009) Electrophysiological correlates of default-mode processing in macaque posterior cingulate cortex. *Proc Natl Acad Sci USA* 106:5948–5953.
27. Miller KJ, Weaver KE, Ojemann JG (2009) Direct electrophysiological measurement of human default network areas. *Proc Natl Acad Sci USA* 106:12174–12177.
28. Parvizi J, Van Hoesen GW, Buckwalter J, Damasio A (2006) Neural connections of the posteromedial cortex in the macaque. *Proc Natl Acad Sci USA* 103:1563–1568.
29. Margulies DS, et al. (2009) Precuneus shares intrinsic functional architecture in humans and monkeys. *Proc Natl Acad Sci USA* 106:20069–20074.
30. Cauda F, et al. (2010) Functional connectivity of the posteromedial cortex. *PLoS* 5:e13107.
31. Immordino-Yang MH, McColl A, Damasio H, Damasio A (2009) Neural correlates of admiration and compassion. *Proc Natl Acad Sci USA* 106:8021–8026.
32. Greicius MD, Krasnow B, Reiss AL, Menon V (2003) Functional connectivity in the resting brain: A network analysis of the default mode hypothesis. *Proc Natl Acad Sci USA* 100:253–258.
33. Seeley WW, et al. (2007) Dissociable intrinsic connectivity networks for salience processing and executive control. *J Neurosci* 27:2349–2356.